

The Gibbs-free-energy landscape for the solute association in nanoconfined aqueous solutions*ZHAO Liang (赵亮),^{1,2} WANG Chun-Lei (王春雷),¹ FANG Hai-Ping (方海平),¹ and TU Yu-Song (涂育松)^{3,†}¹*Division of Interfacial Water and Key Laboratory of Interfacial Physics and Technology, Shanghai Institute of Applied Physics, Chinese Academy of Sciences, Shanghai 201800, China*²*University of Chinese Academy of Sciences, Beijing 100049, China*³*College of Physics Science and Technology, Yangzhou University, Yangzhou 225009, China*

(Received March 4, 2015; accepted in revised form April 20, 2015; published online June 20, 2015)

The theoretical model and the numerical analyses on the Gibbs-free-energy of the association states of amphiphilic molecules in nanoconfined aqueous solutions are presented in detail. We exhibit the continuous change of the Gibbs-free-energy trend, which plays a critical role in the association states of the system transforming from the dispersion state, through the “reversible state”, and finally to the aggregation state in amphiphilic molecule solutions. Furthermore, for the “reversible state”, we present the difference in the free-energy barrier heights of the dispersion state and aggregation state, resulting from the competition between the entropy, which makes the solute molecules evenly disperse in the solution and the energy contribution driving the amphiphilic molecules to aggregate into a larger cluster. These findings provide a comprehensive understanding of confinement effects on the solute association processes in aqueous solutions and may further improve the techniques of material fabrication.

Keywords: Gibbs-free-energy barrier, Dispersion, Aggregation, Nanoconfinement

DOI: [10.13538/j.1001-8042/nst.26.030504](https://doi.org/10.13538/j.1001-8042/nst.26.030504)**I. INTRODUCTION**

The solute association in aqueous solutions plays a fundamental role in various processes, including crystal growth [1, 2], colloid particles nucleation [3, 4], surfactant micellization [5, 6], gas hydrate formation [7, 8], and biomolecule related applications [9–11]. When the confined environment, such as the space between the macromolecules in a cell [12], pores in the soil [13], and nanochannels [14, 15] in man-made nanomaterial, is involved, the solute molecules exhibit different behavior from that in bulk. Zhang *et al.* [16] found that the stability of the native state of the protein can be enhanced at a smaller confinement volume. For the surfactant solutions confined in the nanochannel, various morphologies during the transition appear [17]. The experiment in the confined geometry designed by Julie *et al.* [18] reported that a single skeleton crystal is observed for sodium chloride at a high supersaturation rate.

Our previous work [19] has shown that the pentanol molecules can switch between the dispersion state and the aggregation state, called “reversible state transition”, in nanoconfined aqueous solutions with the aid of molecular dynamics simulations. We built the ideal physical model and numerically calculated the Gibbs-free-energy of a solute with respect to the number of molecules in the cluster. It is found that the unexpected observation is attributed to the two minima separated by a maximum in the Gibbs-free-energy curve under the confinement and existence of a free-energy bar-

rier, which is the same order as the thermal fluctuations. The confinement also leads to the enhancement of the critical aggregation concentration, which results from the fact that the solute number is not sufficient to sustain the stable cluster at a lower concentration in the confined volume.

The pentanol molecule in our MD simulation is described by the Gromos force field, where either a methyl group or ethyl group is considered as a whole group and their hydrogen atoms are implicitly included. This way, the acceleration of computation is evident to track the dynamic association processes, including the dispersion, reversible switch, and aggregation states. The packing of pentanol into clusters is of little influence, as these groups always behave like a whole entity during the aggregation processes, although a rough description of water structures around the methyl or ethyl groups will be obtained because hydrogen atoms on these groups are not explicitly considered.

In this study, we first derive the free-energy formula in terms of the ideal physical model in detail to illustrate the landscape of Gibbs-free-energy of amphiphile association behaviors in the nanoconfined geometry. Secondly, especially for the “reversible state”, we discuss Gibbs-free-energy barriers for the dispersion and aggregation states and numerically investigated the relationship between the Gibbs-free-energy barrier height and the concentration of solute molecules. Finally, the conclusion is summarized based on the characteristic of the “reversible state” of the amphiphilic solute association behavior in nanoconfined aqueous solutions.

II. MODEL AND METHODS**A. Model of the amphiphilic molecule and cluster**

- (1) A single amphiphilic alcohol molecule is modeled by a cuboid with a hydrophilic head and a hydrophobic tail,

* Supported by National Science Fund for Outstanding Young Scholars (No. 11422542), Key Research Program of the Chinese Academy of Sciences (No. KJZD-EW-M03), Knowledge Innovation Program of Chinese Academy Sciences, the High Performance Computing Center of Shanghai University (No. ZQ4000) and Shanghai Supercomputer Center of China.

† Corresponding author, ystu@yzu.edu.cn

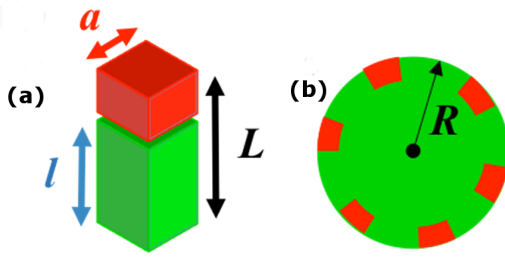


Fig. 1. (Color online) (a) Molecular models for the single amphiphilic molecule and (b) the cluster with a radius R . The cuboids in red and green represent the hydrophilic head ($-\text{CH}_2\text{-OH}$) and hydrophobic tail (alkyl chain). The molecule width and length and the hydrophobic tail length are denoted by a , L , and l , respectively. In the cluster model, the densely packed hydrophobic tails, shown in green, prefer to stay in the interior core and the hydrophilic heads, shown in red, are on the surface. The surrounding water environment is not shown for clarity.

as illustrated by the red and green geometry in Fig. 1(a). The molecule width, molecule length, and tail length are denoted by a , L and l , respectively. The volume of a molecule is $v_m = a^2 L$.

- (2) A cluster consisting of densely packed amphiphilic molecules in water is treated as an ideal spherical aggregate [20] with the radius $R(n)$:

$$R(n) = (3nv_m/4\pi)^{1/3} = (3na^2L/4\pi)^{1/3}, \quad (1)$$

where n is the number of molecules in the cluster, namely, the aggregation number of the cluster. The hydrophobic tails prefer to stay in the interior core and the hydrophilic heads like to occupy the interfacial region exposed to the surrounding water environment, as shown in Fig. 1(b).

B. Methods for Gibbs-free-energy calculations

The theoretical description of Gibbs-free-energy is introduced to calculate the free-energy of amphiphilic solute molecules in nanoconfined aqueous solutions. We considered that only one single cluster is formed and the solute molecule is either in the cluster or dispersed in the solution. The total amount of solute is denoted by N and the number of molecules in dispersion is $N - n$. The Gibbs-free-energy, G , as the function of both the cluster aggregation number, n , and the solute number N , is defined as

$$G(n, N) = \left\{ 4\pi \left(\frac{3v_m}{4\pi} \right)^{\frac{2}{3}} n^{\frac{2}{3}} \cdot \gamma_{\text{hw}\infty} \left[1 - 2\delta_{\text{hw}} \left(\frac{3v_m}{4\pi} n \right)^{-\frac{1}{3}} \right] + na^2\gamma_{\text{w}\infty} \left[1 - 2\delta_{\text{w}} \left(\frac{3v_m}{4\pi} n \right)^{-\frac{1}{3}} \right] - na^2\gamma_{\text{hw}\infty} \left[1 - 2\delta_{\text{hw}} \left(\frac{3v_w}{4\pi} n \right)^{-\frac{1}{3}} \right] + b \cdot \left(\frac{a}{l} \right)^{\frac{4}{3}} k_{\text{B}}Tn^{\frac{5}{3}} - n \cdot |\Delta\mu_{\text{transfer}}| \right\} \cdot \left[k_{\text{B}}T(N - n) \ln \left(\frac{N - n}{V} \right) - k_{\text{B}}T(N - n) + B(N - n) \right], \quad (2)$$

where k_{B} is the Boltzmann constant and T is the system temperature. The first three terms in the curly brace are contributions from the surface energy of hydrophobic tails and the fourth term is from placing the hydrophilic heads onto the cluster surface. The $n \cdot |\Delta\mu_{\text{transfer}}|$ is the free energy difference of transferring a single hydrophobic tail from the dispersed phase into the hydrophobic parts of the cluster. The terms in the square brackets represent the free-energy contribution from the $N - n$ dispersed molecules. $\gamma_{\text{hw}\infty}$ and $\gamma_{\text{w}\infty}$

are the interfacial tension coefficients of hydrophobic tails-water and water-vapor and δ_{hw} , δ_{w} are the corresponding Tolman lengths [20]. The confinement effect is displayed by V , which is the volume, excluding the walls.

The relationship between the aggregation number, n , of the cluster and the amount of solute, N , namely, $n(N)$, can be derived by differentiating the Gibbs-free-energy, $G(n, N)$, to n . The $n(N)$ is given by the relation

$$\left\{ \frac{8\pi}{3k_{\text{B}}T} \left(\frac{3v_m}{4\pi} \right)^{\frac{2}{3}} n^{-\frac{1}{3}} \gamma_{\text{hw}\infty} \left[1 - \delta_{\text{hw}} \left(\frac{3v_m}{4\pi} n \right)^{-\frac{1}{3}} \right] + \frac{\gamma_{\text{w}\infty}}{k_{\text{B}}T} a^2 \left[1 - \frac{4}{3} \delta_{\text{w}} \left(\frac{3v_m}{4\pi} n \right)^{-\frac{1}{3}} \right] - \frac{\gamma_{\text{hw}\infty}}{k_{\text{B}}T} a^2 \left[1 - \frac{4}{3} \delta_{\text{hw}} \left(\frac{3v_w}{4\pi} n \right)^{-\frac{1}{3}} \right] \right\} + b \cdot \frac{5}{3} \left(\frac{a}{l} \right)^{\frac{4}{3}} n^{\frac{2}{3}} + \left(\frac{-|\Delta\mu_{\text{transfer}}| - B}{k_{\text{B}}T} \right) = \ln \left(\frac{N - n}{V} \right), \quad (3)$$

where the terms on the both sides imply the chemical balance between the cluster and other dispersed molecules in the

confined aqueous solutions. By defining the solute concentra-

tion, C , as $C = N/V$, other expressions, $G(n, C)$ and $n(C)$, can be obtained from $G(n, N)$ and $n(N)$ at a certain volume.

To proceed with the numerical calculations, the coefficients are parameterized as follows: $T = 300$ K; $V = 5.0$ nm \times 5.0 nm \times 5.0 nm; For the water, $\gamma_{w\infty} = 72$ mN/m and $\delta_w = 1.23$ Å; For the pentanol molecule, $\gamma_{hw\infty} = 49.53$ mN/m, $a = 2.60$ Å, $l = 5.97$ Å, $b = 0.02$, and $-\left|\Delta\mu_{\text{transfer}}\right| - B = -5.26k_B T$. All of these numerical analyses are achieved by using the Maple 18 software.

With respect to the aqueous solutions solvated with the amount of amphiphilic solute, N , in a certain volume, V , the Gibbs-free-energy, $G(n, N)$ or $G(n, C)$, can be regarded as the function of the aggregation number of the cluster n and thus it is denoted by $G(n)$ for clarity. The local minimum in the Gibbs-free-energy, $G(n)$, is found by

$$\frac{dG(n)}{dn} = 0 \quad \text{and} \quad \frac{d^2G(n)}{dn^2} < 0. \quad (4)$$

Similarly, the local maximum is found by

$$\frac{dG(n)}{dn} = 0 \quad \text{and} \quad \frac{d^2G(n)}{dn^2} > 0. \quad (5)$$

The barrier height, G_{barrier} , is defined by the magnitude of the difference of Gibbs-free-energy values between the local minimum and its adjacent maximum, i.e.,

$$G_{\text{barrier}} = |G_{\text{max}} - G_{\text{min}}|. \quad (6)$$

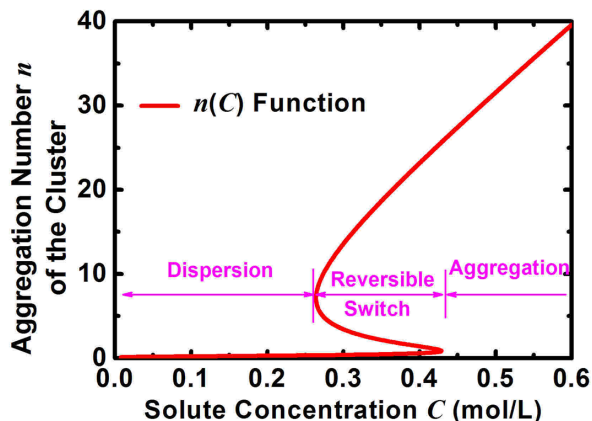


Fig. 2. (Color online) The mathematical picture for the relation, $n(C)$, formulating the dependence of the aggregation number on the cluster, n , on the solute concentration, C .

III. RESULTS

To describe how many solute molecules will aggregate into a cluster and form an association state of the system as the solute concentration increases, we plot the $n(C)$ function in terms of Eq. (3). As shown in Fig. 2, three regions of solute concentration, C , can be recognized. When $C < 0.266$ mol/L, the aggregation number is $n \sim 1$, which indicates no aggregates formed and the solute molecules like to disperse in the solution. When sufficient solute molecules are added into the solution, i.e., $C > 0.425$ mol/L, an evident cluster appears and it grows larger as the solute concentration increases. Interestingly, when 0.266 mol/L $\leq C \leq 0.425$ mol/L in the “reversible

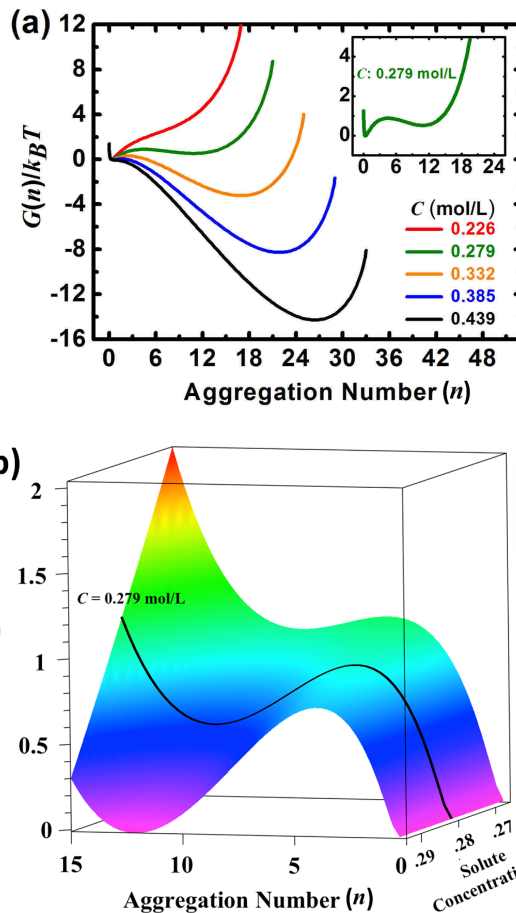


Fig. 3. (Color online) (a) The Gibbs-free-energy, $G(n)$, of the solute molecules in confined aqueous solutions versus the aggregation number of the cluster, n , under various solute concentrations. The subpicture shows the $G(n)$ when $C = 0.279$ mol/L. The $G(n)$ curves are shifted for easy comparison. (b) The landscape of the Gibbs-free-energy with respect to the aggregation number n and solute concentration, C . The surface is colored according to the value of the Gibbs-free-energy.

state”, the solute can exhibit both the dispersion state and the aggregation state, because the three aggregation numbers, n , correspond to a certain solute concentration. This can be seen more clearly in the Gibbs-free-energy landscape in Fig. 3.

In terms of the Gibbs-free-energy formula in Eq. (2) and gradually increasing the solute concentration C , the images of $G(n, C)$ at various C are shown in Fig. 3. For $C = 0.266$ mol/L, there is only one minimum where the aggregation number, $n \sim 1$, corresponding to the dispersion state. For the system with a larger solute concentration of $C = 0.439$ mol/L, the minimum at $n \sim 26$ demonstrates that most of the molecules aggregate together, thus forming a cluster. However, when $C = 0.279$ mol/L, the $G(n)$ displays two minima at $n \sim 1, 12$ separated by a maximum at $n \sim 4$. According to the definitions given by Eq. (4) and Eq. (5), these values correspond to the stable dispersion state, the stable aggregation state, and the metastable state, respectively. This bistability also appears when $C = 0.332$ mol/L and 0.385 mol/L. The continuous change of the Gibbs-free-energy trend with increased solute concentration is more clearly shown in the landscape of the Gibbs-free-energy. Figure 3(b) presents the Gibbs-free-energy landscape with respect to the aggre-

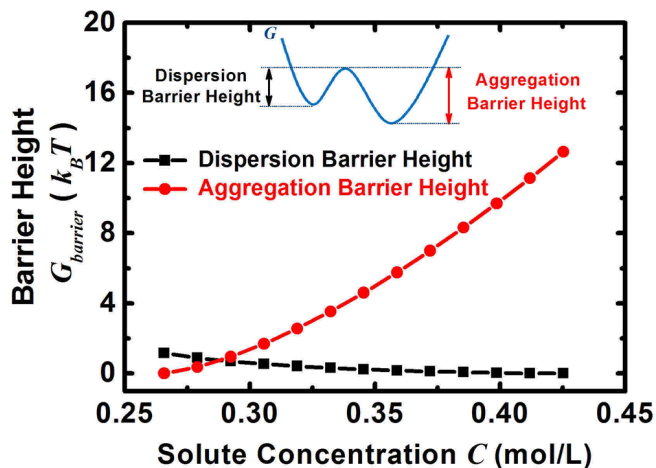


Fig. 4. (Color online) The dependence of the dispersion barrier height and the aggregation barrier height on the solute concentration, C , when the system is in the reversible state.

gation number and the solute concentration. Overall, as the solute concentration, C , increases, the $G(n)$ exhibits the continuous variation that the minimum corresponding to the dispersion state disappears when accompanied by the appearance of the aggregation state.

The emergence of the minima and maximum for the solute concentration $C = 0.279, 0.332$ and 0.385 mol/L in Fig. 3 makes it possible for the system to switch between the dispersion state and the aggregation state by overcoming the free-energy barrier under thermal fluctuations. This activation process at a certain temperature directly relies on the height of barrier. Considering the bistability in the “reversible state” region $0.266 \text{ mol/L} \leq C \leq 0.425 \text{ mol/L}$, the barrier heights for the dispersion state and the aggregation state versus the solute concentration, C , are presented in Fig. 4 by following the definition of the free-energy barrier, G_{barrier} , in Eq. (6).

The max barrier height is the order of hydrogen bond energy

($\sim 8k_B T$) in water at 300 K. That is to say, the transition of solute molecules can occur between these two different states under the thermal fluctuations. Because the energy contribution driving the aggregation dominates the behavior of the solute and the larger cluster owns the lower free-energy, it is seen that the barrier height for the aggregation state rises with the increase of the solute concentration, C . The disappearance of the dispersion energy barrier is probably attributed to the fact that the entropy effect promoting the even distribution of the solute in the solution is reduced.

IV. CONCLUSION

In summary, we presented the detailed derivation of the Gibbs-free-energy landscape and describe the amphiphilic solute association behavior in nanoconfined aqueous solutions. Numerical calculations showed that under the confined geometry, as the solute concentration increases, the solute free-energy curve shows the continuous transition from one minimum with an aggregation number of $n \sim 1$, through two minima separated by one maximum, finally to one minimum where $n \sim N$. This change indicates the system will transit from the stable dispersion state, through the “reversible state”, and finally to the stable aggregation state. In the “reversible state” region, the max energy barrier is the order of the hydrogen bond energy ($\sim 8k_B T$) in water, which allows the system to switch between the dispersion state and the aggregation state. The difference between the free-energy barrier for the dispersion state and the aggregation state is identified. The decrease in the dispersion barrier height and the rise of the aggregation barrier height resulted from the competition between the entropy making the solute evenly distributed in the solutions and the energy contribution driving the solute aggregate into the cluster, as the solute concentration increases.

Our work provides a comprehensive understanding of the confinement on the behavior of solute molecules in aqueous solutions. It is expected that the theory can also be applied to other amphiphilic molecules with more complicated structures, such as peptides or surfactants, in a nanoporous medium or cell, which are widely spread confined environments.

- [1] Piana S, Reyhani M and Gale J D. Simulating micrometre-scale crystal growth from solution. *Nature*, 2005, **438**: 70–73. DOI: [10.1038/nature04173](https://doi.org/10.1038/nature04173)
- [2] Myerson A S and Trout B L. Nucleation from solution. *Science*, 2013, **341**: 855–856. DOI: [10.1126/science.1243022](https://doi.org/10.1126/science.1243022)
- [3] Kraft D J, Ni R, Smallegange F, *et al.* Surface roughness directed self-assembly of patchy particles into colloidal micelles. *P Natl Acad Sci USA*, 2012, **109**: 10787–10792. DOI: [10.1073/pnas.1116820109](https://doi.org/10.1073/pnas.1116820109)
- [4] Chen Q, Whitmer J K, Jiang S, *et al.* Supracolloidal reaction kinetics of Janus spheres. *Science*, 2011, **331**: 199–202. DOI: [10.1126/science.1197451](https://doi.org/10.1126/science.1197451)
- [5] Sanders S A, Sammalkorpi M and Panagiotopoulos A Z. Atomistic simulations of micellization of sodium hexyl, heptyl, octyl, and nonyl sulfates. *J Phys Chem B*, 2012, **116**: 2430–2437. DOI: [10.1021/jp209207p](https://doi.org/10.1021/jp209207p)
- [6] Velinova M, Sengupta D, Tadjer A V, *et al.* Sphere-to-rod transitions of nonionic surfactant micelles in aqueous solution modeled by molecular dynamics simulations. *Langmuir*, 2011, **27**: 14071–14077. DOI: [10.1021/la203055t](https://doi.org/10.1021/la203055t)
- [7] Walsh M R, Koh C A, Sloan E D, *et al.* Microsecond simulations of spontaneous methane hydrate nucleation and growth. *Science*, 2009, **326**: 1095–1098. DOI: [10.1126/science.1174010](https://doi.org/10.1126/science.1174010)
- [8] Debenedetti P G and Sarupria S. Hydrate molecular ballet. *Science*, 2009, **326**: 1070–1071. DOI: [10.1126/science.1183027](https://doi.org/10.1126/science.1183027)
- [9] Hartgerink J D, Beniash E and Stupp S I. Self-assembly and mineralization of peptide-amphiphile nanofibers. *Science*, 2001, **294**: 1684–1688. DOI: [10.1126/science.1063187](https://doi.org/10.1126/science.1063187)
- [10] Shityakov S and Dandekar T. Molecular dynamics simulation of popc and pope lipid membrane bilayers enforced by an intercalated single-wall carbon nanotube. *Nano*, 2011, **6**: 19–29. DOI: [10.1142/s1793292011002317](https://doi.org/10.1142/s1793292011002317)
- [11] Shityakov S, Salvador E, Pastorin G, *et al.* Blood-brain barrier transport studies, aggregation, and molecular dynamics simulation of multiwalled carbon nanotube functionalized with fluorescein isothiocyanate. *Int J Nanomed*, 2015, **10**: 1703–1713. DOI: [10.2147/IJN.S68429](https://doi.org/10.2147/IJN.S68429)
- [12] Homouz D, Perham M, Samiotakis A, *et al.* Crowded, cell-like environment induces shape changes in aspherical protein. *P Natl Acad Sci USA*, 2008, **105**: 11754–11759. DOI: [10.1073/pnas.0803672105](https://doi.org/10.1073/pnas.0803672105)

- [13] Perdrial N, Perdrial J N, Delphin J E, *et al.* Temporal and spatial monitoring of mobile nanoparticles in a vineyard soil: evidence of nanoaggregate formation. *Eur J Soil Sci*, 2010, **61**: 456–468. DOI: [10.1111/j.1365-2389.2010.01263.x](https://doi.org/10.1111/j.1365-2389.2010.01263.x)
- [14] Gardeniers H J G E. Chemistry in nanochannel confinement. *Anal Bioanal Chem*, 2009, **394**: 385–397. DOI: [10.1007/s00216-009-2672-5](https://doi.org/10.1007/s00216-009-2672-5)
- [15] Tu Y S, Xiu P, Wan R Z, *et al.* Water-mediated signal multiplication with Y-shaped carbon nanotubes. *P Natl Acad Sci USA*, 2009, **106**: 18120–18124. DOI: [10.1073/pnas.0902676106](https://doi.org/10.1073/pnas.0902676106)
- [16] Zhang S Q and Cheung M S. Manipulating biopolymer dynamics by anisotropic nanoconfinement. *Nano Lett*, 2007, **7**: 3438–3442. DOI: [10.1021/NI071948v](https://doi.org/10.1021/NI071948v)
- [17] Arai N, Yasuoka K and Zeng X C. Self-assembly of surfactants and polymorphic transition in nanotubes. *J Am Chem Soc*, 2008, **130**: 7916–7920. DOI: [10.1021/ja7108739](https://doi.org/10.1021/ja7108739)
- [18] Desarnaud J, Derluyn H, Carmeliet J, *et al.* Metastability limit for the nucleation of NaCl crystals in confinement. *J Phys Chem Lett*, 2014, **5**: 890–895. DOI: [10.1021/jz500090x](https://doi.org/10.1021/jz500090x)
- [19] Zhao L, Wang C L, Liu J, *et al.* Reversible State Transition in Nanoconfined Aqueous Solutions. *Phys Rev Lett*, 2014, **112**: 078301. DOI: [10.1103/PhysRevLett.112.078301](https://doi.org/10.1103/PhysRevLett.112.078301)
- [20] Prestipino S, Laio A and Tosatti E. Systematic improvement of classical nucleation theory. *Phys Rev Lett*, 2012, **108**: 225701. DOI: [10.1103/PhysRevLett.108.225701](https://doi.org/10.1103/PhysRevLett.108.225701)